J. Plasma Physics (2013), *vol.* 79, *part* 6, *pp.* 1099–1105. © Cambridge University Press 2013
doi:10.1017/S0022377813001128

Signature of gyro-phase drift

MARK E. KOEPKE[1], J. J. WALKER[1], M. I. ZIMMERMAN[2], W. M. FARRELL[2] and V. I. DEMIDOV[1,3]

[1]Department of Physics, West Virginia University, Morgantown, WV, 26506, USA
(mark.koepke@mail.wvu.edu)
[2]Goddard Space Flight Center, National Aeronautics and Space Administration, Greenbelt, MD, 20771, USA
[3]University ITMO, Kronverkskiy pr. 49, St. Petersburg 197101, Russia

(Received 30 August 2013; accepted 6 September 2013)

Abstract. Gyro-phase drift is a guiding center drift that is directly dependent on the charging rate limit of dust grains. The effect of introducing a gyro-phase-dependence on the grain charge leads to two orthogonal components of guiding-center drift. One component, referred to here as grad-q drift, results from the time-varying, gyro-phase angle dependent, *in-situ*-equilibrium grain charge, assuming that the grain charging is instantaneous. For this component, the grain is assumed to be always in its *in-situ*-equilibrium charge state and this state gyro-synchronously varies with respect to the grain's average charge state. The other component, referred to here as the gyro-phase drift, arises from any non-instantaneous-charging-induced modification of the diamagnetic drift and points in the direction of $-\nabla R_{Ld}$ (where R_{Ld} is the grain gyro-radius), i.e. the direction associated with increasing magnitude of *in-situ*-equilibrium charge state. For this component, the grain gyro-synchronously undercharges and overcharges with respect to its gyro-synchronously varying, *in-situ*-equilibrium charge state. These characteristics are illustrated with a single-particle code for predicting grain trajectory that demonstrates how gyro-phase drift magnitude and direction could be exploited, using an extended version of the presented model, as sensitive indicators of the charging time of dust grains because of the cumulative effect of the ever-changing charge state of a grain making repeated excursions in inhomogeneous plasma over many gyro-periods.

1. Introduction to gyro-phase drift

Plasma, free electrons and ions (typically charged singly and positively) that behave classically and collectively via the long-range electromagnetic force, meets the criteria that the Debye-shielding scale length is both much larger than the interparticle spacing and much smaller than the plasma dimensions. Plasma is considered dusty if it contains relatively massive particulates (e.g. dust grains) with net charge. An electrostatic potential well, arising naturally in the plasma or applied externally, can confine the dust grains and the properties of this dusty plasma equilibrium and its dynamics can be studied. The dusty plasma is considered magnetized if the charge-to-mass ratio of the dust grain is sufficiently large that a significant fraction of the grains gyrate with gyro-radii much smaller than the dusty plasma's dimensions perpendicular to the magnetic field and if the dust gyro-motion is not prevented by particle collisions. For the magnetized-orbit case, the confinement of grains is ruined by the influence of an electrostatic potential well, due to finite-gyro-radius effects, unless grain size and radial electric field are kept small.

The gyro-phase drift is one of the drift motions, e.g. $\boldsymbol{E} \times \boldsymbol{B}$ drift, magnetic-gradient drift, and field-line-curvature drift, that results from gyro-averaging the equation of motion for the dust grain in the frame that co-rotates with the planet or moon. The original goal for investigating gyro-phase drift was a complete description of all guiding center drifts of a dust grain orbiting a planet or moon (Northrop and Hill 1983). Goree (1994) estimated the time for a dust grain to charge up from zero elementary charges to one e-folding of the *in-situ*-equilibrium value in a homogeneous plasma as $k_T T_e^{1/2}/(an_0)$, where T_e is the electron temperature in eV, a is the dust grain radius in meters, n_0 is the plasma density in m^{-3}, and k_T is a given function of both T_i/T_e and m_i/m_e in units of seconds $\mathrm{m}^{-2}\mathrm{eV}^{-\frac{1}{2}}$, which is fit to a numerical model. The normalized charging rate $\frac{1}{q}\frac{\mathrm{d}q}{\mathrm{d}t}$ is the inverse of the charging time.

Gyro-phase drift is a guiding center drift that is directly dependent on the limited charging rate of dust grains. The effect of introducing a gyro-phase-dependence on the grain charge leads to two orthogonal components of guiding-center drift that, in the absence or presence of an electric field, could be combined into a single gyro-phase drift vector and treated separate from $\boldsymbol{E} \times \boldsymbol{B}$ drift. One component, referred to here as grad-q drift, results from the time-varying, gyro-angle dependent, *in-situ*-equilibrium grain charge, assuming that the grain charging is instantaneous, and is aligned or anti-aligned with the $\boldsymbol{E}\times\boldsymbol{B}$ direction if the self-consistent electric field $\boldsymbol{E}$ were non-zero. The other component, referred to here as the gyro-phase drift, arises from any non-instantaneous-charging-induced modification of the diamagnetic drift (see equation (8) of Northrop and Hill (1983) and figure 9 on page 71 of Bliokh et al. (1994)), and points in the direction of increasing magnitude of *in-situ*-equilibrium charge state. The gyro-phase drift magnitude and direction between gyro-phase and grad-q drifts are sensitive indicators of the charging time of dust grains because of the cumulative effect of the ever-changing charge state of a grain making repeated excursions in inhomogeneous plasma. To further clarify, the grad-q drift, arising from the assumption that the grain is always in its *in-situ*-equilibrium charge state and that this state is gyro-synchronously varying with respect to the grain's average charge state, will be labeled separately from the gyro-phase drift component that arises solely from the fact that the grain can be gyro-synchronously undercharged or overcharged with respect to its gyro-synchronously varying *in-situ*-equilibrium charge state.

2. Space realization of magnetized-orbit dusty plasma

Small dust grains exist near Saturn (Gurnett et al. 1983) and make up the bulk of Jupiter's gossamer ring (Northrop et al. 1989). Such small grains are easily magnetized and, due to their gyromotion, exhibit orbit-radial oscillations in their orbital trajectory around the planet. A charging/de-charging cycle is experienced by the grain if the radial oscillations traverse regions of different electrostatic potential and/or charged-particle flux. Gyro-phase shifts between the grain charging cycle and the cycle associated with the instantaneous grain surface potential are caused by the finite charging rate and result in a modification to the usual $\boldsymbol{E}\times\boldsymbol{B}$ drift. This modification, known as gyro-phase drift, is in the orbit-radial direction (Goertz and Morfill 1983; Northrop and Hill 1983; Bliokh and Yarashenko 1985). This drift can be observed only in a magnetized dusty plasma. For simple planet-encircling orbits with no gyro-motion, the gyro-phase drift does not exist. This gyro-phase drift is distinct from the (gravitational-centrifugal force-balance induced) radial drift that exists for unmagnetized grains located inside or outside the synchronous-orbit distance from the planet.

On December 31, 2000, Cassini had a closest approach with Jupiter and made simultaneous measurements with Galileo. The dust-grain fluxes seen by the two satellites were comparable even though Galileo was closer to Io, a significant source of dust. These measurements imply that there must be processes, yet to be modeled, energizing dust particles as they cross outer parts of the Jovian magnetosphere. As grains are ejected from the moon's surface by meteor impacts, they pass through Jupiter's magnetosphere and get charged. The smallest grains detected in the vicinity of Jupiter exhibit collimated beam properties. The dust streams are directed such that the tangential component of interplanetary magnetic field plays a role, and indeed, a correlation between the stream component and the tangential component of magnetic field is observed. A mechanism for sweeping charged submicron dust away from Io, or one of the other Jovian moons, involving the Lorentz force, affects any grains small enough to become magnetized, and may be responsible for the directionality of these beams (Grün et al. 1993; Horanyi et al. 1993).

3. Laboratory realization of magnetized-orbit dusty plasma

Amatucci et al. (2004) reported dust gyro-motion in a 0.46-m-diameter, glow-discharge, argon plasma: $a_\mu = 1.2$, $m_d = 2.5\times10^{-16}$ kg, $V_d = 70$ V, $q_d = 4\times10^{-15}$ C, $B = 0.25$ T, $k_B T_e = 100$ eV for primary electrons and $k_B T_e < 1.6$ eV for plasma electrons, $T = 300$ K for both ions and dust grains, $n_i = 10^{16}\,\mathrm{m}^{-3}$, $v_{d,0,\perp} = 2-8\times10^{-3}\,\mathrm{m\,s^{-1}}$, $\omega_{cd} = 2.2-4.7\,\mathrm{rad\,s^{-1}}$ (or $f_{cd} = 0.4-0.9$ Hz), and $r_{cd} = 0.5-2$ mm. Thus the feasibility of observing magnetized-orbit grains large enough to image with particle-image velocimetry (PIV) is implied. Experiments that use grains too small to image with PIV require probe techniques established by Barkan et al. (1994). The new Auburn Magnetized Dusty Plasma Experiment (MDPX) device is under construction and experimental operations are expected to begin in 2014. The $\boldsymbol{E}\times\boldsymbol{B}$ drift is large unless the plasma potential's radial profile is restricted to be shallow and have a small extreme value. Figure 1 shows how the ambient radial electric field enlarges the effective gyro-radius of dust grains in a cylindrical chamber like the Auburn MDPX. If the neutral atom-to-charged grain drag force is not too large, the gyro-phase drift in Auburn's MDPX and, hence, the rate of charging for various dust-grain materials might be measurable. The body of theoretical work on charging rates that is being used in basic-physics, industrial-physics, and astrophysics applications has only a limited degree of experimental confirmation, especially on the subject of non-stationary dust-grain charging.

Normally, uncertainty in the measurement of dust-grain charge is sufficiently large to dominate all other uncertainties in interpreting dusty-plasma behavior (Konopka and Morfill 2003). The most precise method to determine dust-grain charge, based on the analysis of direct particle collisions, is approximately 20% uncertain. Methods based on observing the vertical resonance frequency of particles levitated in an electric field can be 50% uncertain. Fitting a measured dusty-plasma waves dispersion to theoretically determined curves is considered 20%–50% uncertain. The accuracy of some of these methods is limited by assumptions of a relationship between the fitting parameter for the charge and the Debye screening parameter. Some methods rely on an approximate sheath model. In many cases, flowing ions and trapped ions are not taken into account so that values represent effective charge only. Without alternatives

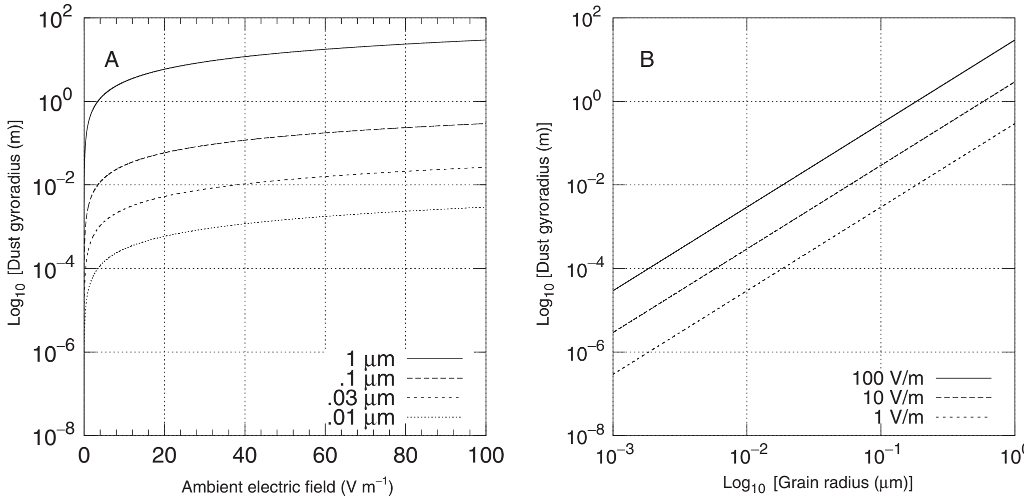

Figure 1. The effective gyro-radius can be accommodated in a laboratory vacuum vessel only for small magnitude of radial electric field and small grain radius. A: Effective dust grain gyro-radius as a function of a constant, ambient electric field is plotted for grain diameters $a = 1\,\mu$m, $a = 0.1\,\mu$m, $a = .015\,\mu$m, and $a = 0.01\,\mu$m. B: Effective gyro-radius as a function of grain radius is plotted for constant, ambient electric field values of $100\,\text{V m}^{-1}$, $10\,\text{V m}^{-1}$, and $1\,\text{V m}^{-1}$.

for measuring charging rates, these same uncertainties will continue to restrict the precision of charging-rate measurements. Since different charging models can be indistinguishable given a 20%–50% margin, there is a need for attaining better than 10% precision in charge and charging measurements. This precision is conceivable with improved physical insight into charging and discharging processes associated with grains at the nanometer, micrometer, and millimeter scale. The capability to monitor both the gyro-phase drift motion and the wave-spectral feature of dust cyclotron waves in the ensemble of individual grains would supply important laboratory experimental evidence for validating grain-charging models. Spatially or temporally modulating the plasma potential or charged-particle flux would induce charge and electron temperature changes for interpretting cause and effect.

With cylindrical geometry in laboratory experiments on magnetized-orbit dust, the radial profile of plasma potential must be adjusted to control the confinement of charged grains. An investigation of the $\boldsymbol{E} \times \boldsymbol{B}$ drift, total diamagnetic drift, and gyro-phase drift may be carried out as $\boldsymbol{E}(\boldsymbol{r})$ is adjusted but note that the gyro-phase drift signal, perpendicular to the other two drifts, represents an uncontaminated signature of non-stationary charging mechanisms. Measurements of gyro-phase drift associated with dust-grain materials having different charging attributes would then be possible.

4. Dusty-plasma parameters that affect grain-charging rate

The plasma parameters associated with dusty-plasma laboratory experiments extend from the collisionless to very collisional regimes. Typically, a specific method for producing plasma, usually identified by the generic name of the plasma device (e.g. Q-machine discharge, radio-frequency discharge, dc glow discharge, helicon discharge), corresponds to a narrow collisionality subrange. Amatucci et al. (2004) report the following plasma parameters for their dusty plasma experiment in which a few of the grains were magnetized: plasma density $= 10^{10}\ \text{cm}^{-3}$, electron temperature $= 1.6$ eV, room-temperature argon-ion plasma, 220 mTorr room-temperature neutral argon background gas, magnetic field strength $= 0.25$ T, ion-neutral collision frequency is 12 times the angular frequency of ion gyration, and a dc glow discharge plasma. Auburn's MDPX is expected to have the following parameters: plasma density $= 10^{10}\ \text{cm}^{-3}$, electron temperature $= 1.6$ eV, room-temperature argon-ion plasma, $\leqslant$220 mTorr room-temperature neutral argon background gas, magnetic field strength $= 4$ T, ion-neutral collision frequency is 0.12 times the angular frequency of ion gyration, and a hybrid RF/DC discharge plasma.

Dust grains charge by bombardment of the grain surface by background-plasma electrons and ions, photo-electron emission by ultraviolet radiation, ion sputtering, secondary electron production, and other processes less relevant to the proposed research. In low-temperature laboratory plasmas, grains are almost always negatively charged (V_d<0) such that the grain's surface electrostatic potential (in volts) is equal to the difference between the floating potential V_f and the space potential V_s of the plasma. Surface potential V_d is determined by the condition that collected electron current is equal to collected ion current, and thus depends on the ion-electron ratios of mass, temperatures, and density.

5. Numerical approach to charge collection to spherical granule

We compute the single-grain trajectory in a dust-absent plasma using a stationary inertial lab frame. In this

https://doi.org/10.1017/S0022377813001128 Published online by Cambridge University Press

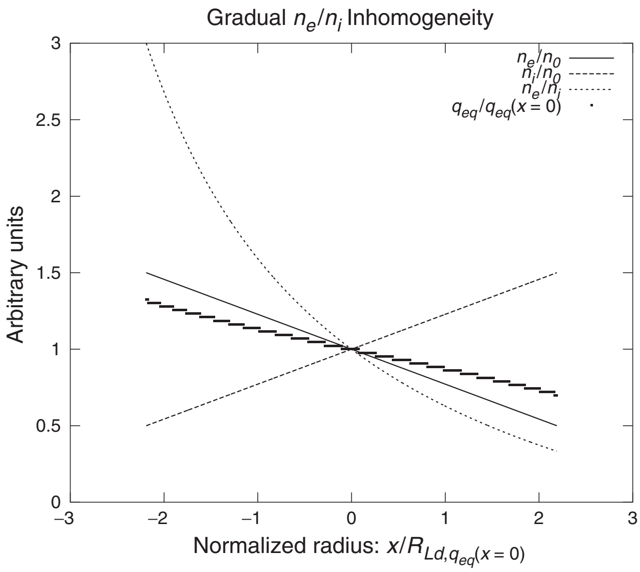

Figure 2. Profile used for the simulations. The electron and ion densities, n_e, n_i, are normalized to $n_0 = 10^{16}\,\mathrm{m}^{-3}$. The ratio n_e/n_i is also plotted, as is the dimensionless quantity $q_{eq}(x)/q_{eq}(x=0)$, which is proportional to the number of electrons on the grain. The discrete steps of $q_{eq}(x)/q_{eq}(x=0)$ correspond to an addition or subtraction of one electron. The abscissa is scaled to the gyro-radius corresponding to the equilibrium charge of a 0.015 μm radius grain at $x=0$, which is 43 electrons ($R_{Ld}(t=0) = 0.572$ mm).

paper, we examine the case of a gradually varying ratio between ion and electron density, as shown in Fig. 2, with each species characterized by a Maxwellian velocity distribution having a temperature T_i and T_e, respectively. An adjustable charge increment parameter, α, is used to control charge evolution much like how a decreased or increased density changes charge evolution. Unlike in Northrop's case, we examine a laboratory relevant scenario where the dust thermal speed is much smaller than the ion thermal speed. In this case, the electric field in the plane of the gyro-motion is taken to be zero. The ion drag force, neutral drag force, gravitational force, and other typical forces on a dust grain are ignored for simplicity. The magnetic field is 4 T. We assume room-temperature ions ($T[Ar^+] = 0.0025$ eV) and atoms and 1.6 eV temperature electrons for the sake of modeling the Auburn MDPX (Thomas et al. 2012). The initial grain speed was oriented in the inhomogeneity direction. We also used $n_0 = 10^{16}\ \mathrm{m}^{-3}$ as the background density for $a = 0.015\,\mu$m radius dust grains.

A symplectic, leapfrog integrator is used to solve the equations of motion resulting from the Lorentz force (Walker et al. 2013). Since $R_{Le,i} > a$ for our choice of parameters, the unmagnetized currents is used. For $q < 0$, and for dust grain speeds much less than the ion thermal velocity, these currents are:

$$\begin{aligned} I_e &= -e4\pi a^2 n_e \frac{v_{th,e}}{2\sqrt{\pi}} \exp\left(\frac{eq}{Ck_bT_e}\right), \\ I_i &= e4\pi a^2 n_i \frac{v_{th,i}}{2\sqrt{\pi}} \left(1 - \frac{eq}{Ck_bT_i}\right), \end{aligned} \tag{5.1}$$

where $v_{th,e,i} = \sqrt{\frac{2k_bT_{e,i}}{m_{e,i}}}$, $n_e = n_i = n_0$, $V_{space} - V_{surface} = q/C$, and $C = 4\pi\epsilon_0 a$ is the grain capacitance. With these currents specified, the charge on the grain can be updated during each charging timestep by $q_{n+1} = q_n + \Delta q_n$, where $\Delta q_n = \frac{I_e+I_i}{\Delta t}$ is the n^{th} charge update. Controlling the charging rate of the dust grain is a key feature of this model, since gyro-phase drift depends on the charging rate.

The charging rate for our set of parameters suggests that the grain is fully charged in $\sim \mu$s, while the gyro-period is ~ 3 ms. For charging time much less than gyro-period, the grain charges to the *in-situ*-equilibrium charge at each spatial location during a gyro-orbit. There should still be a grad-q drift, but no gyro-phase drift for $a = 0.015\,\mu$m, $n_0 = 10^{16}\,\mathrm{m}^{-3}$, and $\alpha = 1$. To arbitrarily control the grain charging and force the charging to not be instantaneous, an adjustable charging parameter, α, is used in the following way: $q_{n+1} = q_n + \Delta q_n'$, where $\Delta q_n' = \alpha\Delta q_n$. For $\alpha = 1$, the dust grain charges without restriction. For $a = 0.015\,\mu$m, $n_0 = 10^{16}\,\mathrm{m}^{-3}$, and $\alpha = 1$, the charging time is less than the gyro-period and $\alpha < 1$ is used to artificially delay the achievement of *in-situ*-equilibrium charge state when plasma conditions change. If $\alpha = 0$, then the dust grain charge effectively never changes, no matter how large the current may be to

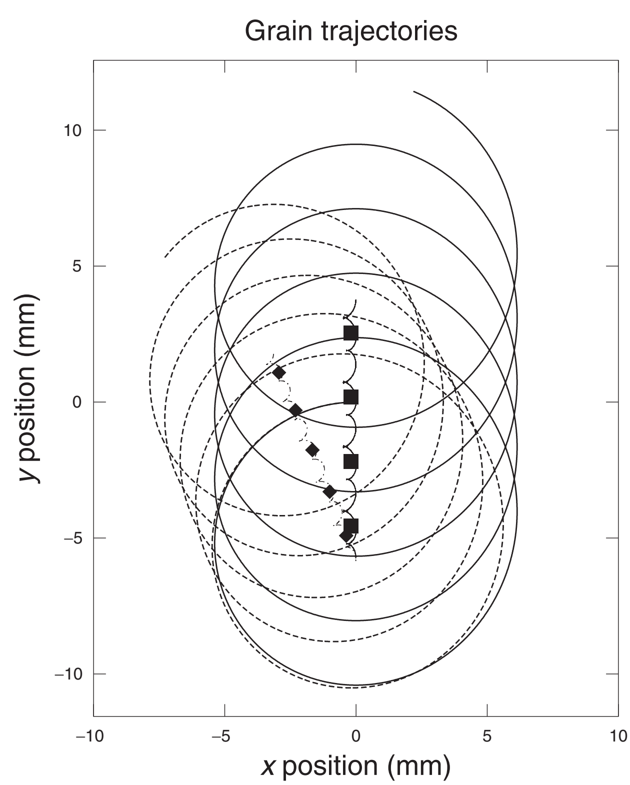

Figure 3. Grain trajectories for $a = 0.015\,\mu$m and $\boldsymbol{B} = B\hat{z}$, where $B = 4$ T. The dashed and solid lines correspond to a charging rate parameter of $\alpha = 1$ and $\alpha = 0.0105$ respectively. Squares and diamonds indicate the gyro-averaged guiding centers of the trajectories for $\alpha = 1$ and $\alpha = 0.0105$, respectively. The instantaneous guiding centers are represented by the solid ($\alpha = 1$) and dashed ($\alpha = 0.0105$) helical lines.

https://doi.org/10.1017/S0022377813001128 Published online by Cambridge University Press

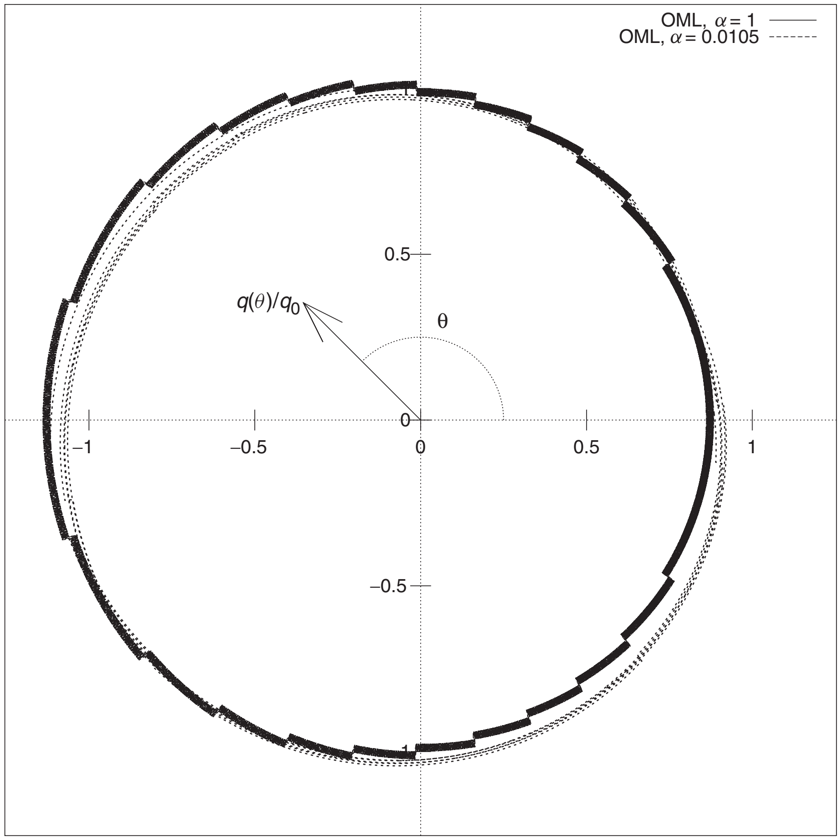

Figure 4. Radial distance from origin is grain charge normalized to the instantaneous *in-situ*-equilibrium grain charge ($q_0 = -43e$, in this case) as a function of gyro-angle for $\alpha = 1$ (solid line) and $\alpha = 0.0105$ (dashed line). Lines appear thickened because multiple gyro-periods are displayed and gyro-phase angle at which single-electron charging events occur are not unique and because the thickness reflects charge fluctuation $+1, -0$ electron. The gyro-angle $\theta = 0$ refers to the $+\hat{x}$ axis here.

the dust grain. It should be noted that the numerical method does not assume any particle drifts or charge modulation of the dust grain *a priori*; the integrator solves the equation of motion of the dust grain resulting from the Lorentz force during the Newtonian time step while it computes the ion and electron currents, which are both functions of the dust grain charge, i.e. dust grain surface potential, at each charging timestep. For the Newton time step, 2000 points per gyrocycle is used.

6. Predictions of gyro-phase drift and simulation results

Figure 3 shows a comparison of different grain trajectories for the gradual n_e/n_i inhomogeneity (Fig. 2) using the OML model with instantaneous ($\alpha = 1$) and non-instantaneous ($\alpha = 0.0105$) grain charging. All trajectories are started at $x = 0$, $y = 0$, with an initial velocity of $v_x = -11$, $v_y = 0$ (in units of m s^{-1}). Also at $t = 0$, the particle charge and gyro-radius for this dust grain was −43e and 5.7 mm, respectively. The grain is initialized with the *in-situ*-equilibrium charge in order to avoid complications involved with the transient effects from the grain starting with no electrons on it. The trajectory of the instantaneous gyro-centers are also plotted, which are represented by the helical lines having smaller radial excursions than the actual grain trajectories.

With no charge delay ($\alpha = 1$), the dust grain experiences the grad-q drift only, whereas a charge delay of $\alpha = 0.0105$ results in a grain that experiences both the grad-q drift and gyro-phase drift. As evident in Fig. 3, the grad-q drift is along the $-\nabla q_{eq}/q_{eq} \times \boldsymbol{B}$ direction. The grad-q drift (Bliokh et al. 1994), assuming that the grain charges instantaneously ($\alpha = 1$), takes the form:

$$\boldsymbol{v}_{\nabla q} = -\text{sign}(q_{eq}) \frac{m_d v_\perp^2 \frac{\partial q_{eq}}{\partial x}}{q_{eq}^2 B^2} \hat{y}, \tag{6.1}$$

where q_{eq} is the *in-situ*-equilibrium grain charge at the gyro-center, and $\frac{\partial q_{eq}}{\partial x}$ is evaluated at $x = x_{gc}$, with x_{gc} being the x-component of the guiding center position. For the inhomogeneity used (Fig. 2), if the step-like nature of q_{eq} is approximated as a continuous function, q_{eq} is a nearly linear function of x, and so $\frac{\partial}{\partial x} q_{eq}$ can be treated as a constant ($\sim 1.6 \times 10^{-16}$C m^{-1}). For a grain with $\alpha = 1$, this results in a predicted grad-q drift of 0.369 m s^{-1}, while the value obtained from gyro-averaging the trajectories from the simulation was 0.726 m s^{-1}. This discrepancy in predicted values might be a result of simplifications in the gyro-averaging.

https://doi.org/10.1017/S0022377813001128 Published online by Cambridge University Press

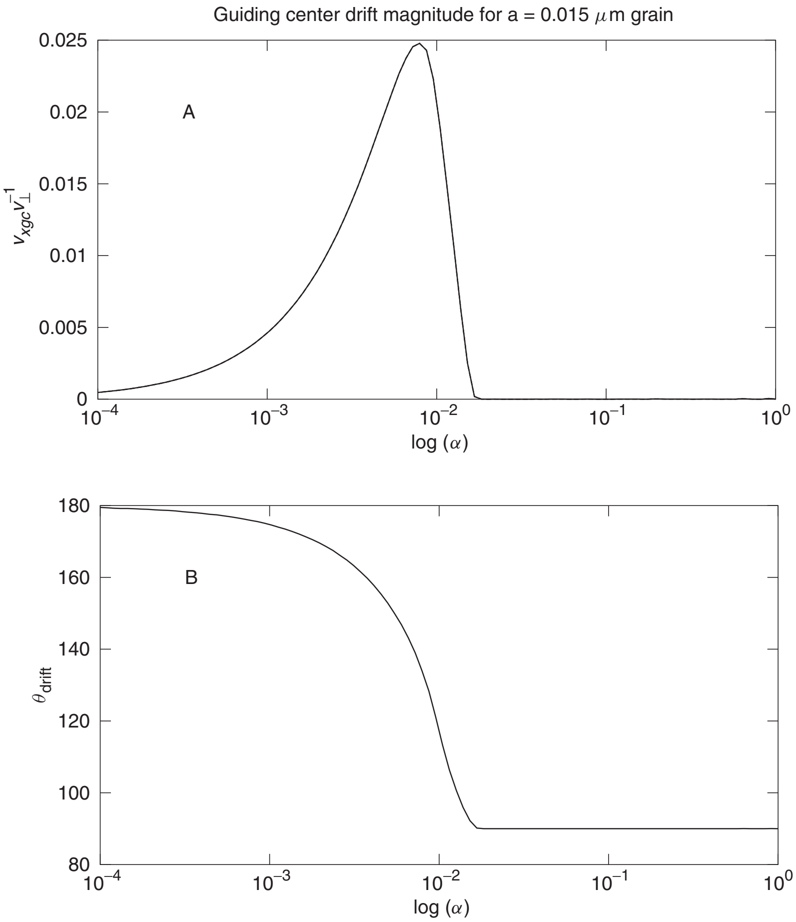

Figure 5. Gyro-phase drift magnitude and direction dependence on the adjustable charge-rate parameter α. A: The magnitude is normalized by the perpendicular velocity, $v_\perp = 11\,\text{m s}^{-1}$. B: The angle θ_{drift}, in degrees, is relative to the $\hat{x}$ direction. An angle of 180° corresponds to a drift direction that is entirely along the $-\hat{x}$, and an angle of 90° corresponds to a drift direction that is entirely along the $\hat{y}$ direction. Above $\alpha = 0.02$, no gyro-phase drift occurs for this case. Below $\alpha = 10^{-4}$, neither gyro-phase nor grad-q drift occurs for this case.

The grain charge as a function of gyro-phase for the two different trajectories in Fig. 3 is shown in Fig. 4. For both trajectories, the grain charge at each gyro-angle is normalized by the *in-situ*-equilibrium grain charge that the same grain would attain at the instantaneous gyro-center corresponding to this gyro-angle $(q(\theta)/q_{eq}(x = x_{gc}(t)))$. A grain having a fixed grain charge in gyro-phase would be displayed as a circle with radius of 1 in this kind of plot. The evolution of particle charge is tracked for approximately five gyro-periods. For the $\alpha = 1$ trajectory, the resulting plot in gyro-angle is nearly circular in shape, although its center is offset from the origin, as expected for the inhomogeneous-plasma case. For $\theta = 0$, the grain has the fewest number of electrons during a gyro-orbit, and for $\theta = \pi$, the grain is maximally charged negatively during a gyro-orbit. The discrete steps apparent in this plot, which yields a circular sawblade-like appearance, are representative of a net loss or a gain of one electron from the previous, discrete, circular-arc step. Additionally, between these sudden transitions, the grain continuously gains and loses an electron, causing its charge state to fluctuate rapidly between each new pair of neighboring charge states. This fluctuation increases the line thickness $\delta q = |q_{n+1} - q_n|$ to be a single $\pm$ element change e. During each gyro-cycle, the same pattern is retraced in the q versus gyro-phase angle plot for a dust grain having $\alpha = 1$. The choice of initial gyro-phase does change the *in-situ*-equilibrium charge at the guiding center q_0, but it does not appreciably alter the plots in Fig. 4.

In contrast, for the $\alpha = 0.0105$ polar plot in Fig. 4, the same pattern is not retraced for each gyro-cycle. If both $\alpha = 1$ and $\alpha = 0.0105$ grains start at $\theta = \pi/2$ in gyro-phase, the $\alpha = 0.0105$ grain will subsequently become undercharged with respect to $\alpha = 1$ as both grains follow trajectories in physical space that go into increasingly non-neutral (negative) plasma. As θ increases past $\theta = \pi$, both grains are leaving the region where the n_e/n_i ratio is highest. However, because the $\alpha = 0.0105$ grain does not immediately reach the *in-situ*-equilibrium, it stays undercharged with respect to $\alpha = 1$ past $\theta = \pi$, reaching a maximum value at $\theta = 200°$ with standard deviation of 9° in Fig. 4. This maximum charge state for the $\alpha = 0.0105$ grain is between the $\theta = \pi$ charge states of the two grains. The $\alpha = 0.0105$ grain is now overcharged with respect to $\alpha = 1$ after $\theta = 200°$. For $\theta > \frac{3}{2}\pi$,

https://doi.org/10.1017/S0022377813001128 Published online by Cambridge University Press

both grains are entering the region where the n_e/n_i ratio is decreasing, and are becoming less negatively charged. The $\alpha = 0.015$ grain does not immediately reach the lower *in-situ*-equilibrium charge state, achieving its smallest charge state when the two grains again match, at $\theta \sim 20^\circ$ with a standard deviation of 1°. The capacitive effects of grain charging that are inherently present in the OML model ensure that the dust grain never reaches the *in-situ*-equilibrium charge during a gyro-orbit if the charging rate is low enough, as is qualitatively demonstrated in Fig. 5.

The magnitude of the gyro-phase drift velocity and the direction with respect to the inhomogeneity direction varies with the value of the charge delay parameter (α), reaching a peak near 10^{-2} (Fig. 5). When the grain has no delay ($\alpha = 1$), it charges to the *in-situ*-equilibrium charge much faster than it completes a gyro-orbit, so there is no modification to the particle trajectory beyond the effect of the grad-q drift (which is an effect arising only from gyro-synchronous charge variation). As α is lowered, the gyro-phase drift reaches a peak when the charging timescale is comparable to the gyro-period timescale (Walker et al. 2013). As α is further lowered, the grain changes charge state sufficiently slowly during a gyro-orbit that it does not change charge state enough during a gyro-orbit that negligible modification of the $\alpha = 1$ gyro-motion occurs and both gyro-phase and grad-q drift vanish. This is reflected in Fig. 5, in that the gyro-phase drift magnitude steadily decreases and the direction of the guiding center drift approaches $\theta_{\text{drift}} = \pi/2$ (using the same polar coordinates), as α is lowered beyond $\alpha = 10^{-2}$, consistent with the grad-q drift also steadily decreasing.

The gyro-phase drift is a direct consequence of the non-stationary charging process of dust grains when q_{eq} is spatially inhomogeneous, as demonstrated in Figs. 3–5. Non-stationary charging has been previously demonstrated to be important in laboratory conditions (Nunomura et al. 1999).

Acknowledgements

Funding through the U.S. Department of Energy, Office of Fusion Energy Science grant DE-SC0001939 and useful discussions with Dr. Marlene Rosenberg are gratefully acknowledged.

References

Amatucci, W. E., Walker, D. N., Gatling, G. and Scime, E. E. 2004 Direct observation of microparticle gyromotion in a magnetized direct current glow discharge dusty plasma. *Phys. Plasmas* **11**(5), 2097–2105.

Barkan, A., D'Angelo, N. and Merlino, R. L. 1994 Charging of dust grains in a plasma. *Phys. Rev. Lett.* **73**, 3093–3096.

Bliokh, P., Sinitsin, V. and Yaroshenko, V. 1994 *Dusty and Self-Gravitational Plasmas in Space*. Dordrecht, The Netherlands: Kluwer.

Bliokh, P. V. and Yarashenko, V. V. 1985 Electrostatic waves in saturn's rings. *Sov. Astron.* **43**, 330–336.

Goertz, C. K. and Morfill, G. 1983 A model for the formation of spokes in saturn's ring. *Icarus* **53**(2), 219–229.

Goree, J. 1994 Charging of particles in a plasma. *Plasma Sources Sci. Technol.* **3**(3), 400.

Grün, E. et al. 1993 Discovery of Jovian dust streams and interstellar grains by the ulysses spacecraft. *Nature* **362**, 428–430.

Gurnett, D. A., Grün, E., Gallagher, D., Kurth, W. S. and Scarf, F. L. 1983 Micron-sized particles detected near saturn by the voyager plasma wave instrument. *Icarus* **53**(2), 236–254.

Horanyi, M., Morfill, G. and Grün, E. 1993 Mechanism for the acceleration and ejection of dust grains from jupiter's magnetosphere. *Nature* **363**, 144–146.

Konopka, U. and Morfill, G. 2003 Magnetic field driven effects in complex plasmas. In *International Topical Conference on Plasma Physics*. Santovini, Greece. 8–12 September 2003.

Northrop, T. G. and Hill, J. R. 1983 The adiabatic motion of charged dust grains in rotating magnetospheres. *J. Geophys. Res. Space Phys.* **88**(A1), 1–11.

Northrop, T. G., Mendis, D. A. and Schaffer, L. 1989 Gyrophase drifts and the orbital evolution of dust at jupiter's gossamer ring. *Icarus* **79**(1), 101–115.

Nunomura, S., Misawa, T., Ohno, N. and Takamura, S. 1999 Instability of dust particles in a coulomb crystal due to delayed charging. *Phys. Rev. Lett.* **83**, 1970–1973.

Thomas, E., Merlino, R. L. and Rosenberg, M. 2012 Magnetized dusty plasmas: the next frontier for complex plasma research. *Plasma Phys. Control. Fusion* **54**(12), 124034.

Walker, J. J., Koepke, M. E., Zimmerman, M. I., Farrell, W. M. and Demidov, V. I. 2013 Analytical model for gyro-phase drift arising from abrupt inhomogeneity. *J. Plasma Phys*. (To appear).